Brain Temperature Measured by Using Proton MR Spectroscopy Predicts Cerebral Hyperperfusion after Carotid Endarterectomy[1]

Toshiyuki Murakami, MD
Kuniaki Ogasawara, MD
Yoshichika Yoshioka, PhD
Daiya Ishigaki, MD[2]
Makoto Sasaki, MD
Kohsuke Kudo, MD
Kenta Aso, MD
Hideaki Nishimoto, MD
Masakazu Kobayashi, MD
Kenji Yoshida, MD
Akira Ogawa, MD

Purpose: To determine whether brain temperature measured by using preoperative proton magnetic resonance (MR) spectroscopy could help identify patients at risk for cerebral hyperperfusion after carotid endarterectomy (CEA).

Materials and Methods: Institutional review board approval and informed consent were obtained. Acquisition of proton MR spectroscopic data by using point-resolved spectroscopy without water suppression was performed before CEA in the bilateral cerebral hemispheres of 84 patients with unilateral internal carotid artery stenosis (≥70%) and without contralateral internal carotid artery steno-occlusive disease. Brain temperature was calculated from the chemical shift difference between water and *N*-acetylaspartate signals at proton MR spectroscopy. Cerebral blood flow (CBF) was also measured by using single photon emission computed tomography and *N*-isopropyl-*p*-[^{123}I]-iodoamphetamine before and immediately after CEA and on the 3rd postoperative day. The relationship between each variable and the development of post-CEA hyperperfusion (CBF increase ≥ 100% compared with preoperative values) was evaluated with univariate statistical analysis followed by multivariate analysis.

Results: A linear correlation was observed between preoperative brain temperature difference (the value in the affected hemisphere minus the value in the contralateral hemisphere) and increases in CBF immediately after CEA ($r = 0.763$ and $P < .001$) when the preoperative brain temperature difference was greater than 0. Cerebral hyperperfusion immediately after CEA was observed in nine patients (11%). Elevated preoperative brain temperature difference was the only significant independent predictor of post-CEA hyperperfusion. When elevated brain temperature difference was defined as a marker of hemodynamic impairment in the affected cerebral hemisphere, use of preoperative brain temperature difference resulted in 100% sensitivity and 87% specificity, with a 47% positive predictive value and a 100% negative predictive value for the prediction of post-CEA hyperperfusion. Hyperperfusion syndrome developed on the 3rd and 4th postoperative days in two of the nine patients who exhibited hyperperfusion immediately after CEA.

Conclusion: Brain temperature measured by using preoperative proton MR spectroscopy may help identify patients at risk for post-CEA cerebral hyperperfusion.

[1] From the Department of Neurosurgery (T.M., K.O., D.I., K.A., M.K., K.Y., A.O.) and Advanced Medical Research Center (Y.Y., M.S., K.K., H.N.), Iwate Medical University, 19-1 Uchimaru, Morioka 020-8505, Japan. Received May 27, 2009; revision requested July 15; revision received September 18; accepted October 7; final version accepted March 30, 2010. Supported in part by Core Research for Evolutional Science and Technology of Japan Science and Technology Agency. **Address correspondence to** K.O. (e-mail: *kuogasa@iwate-med.ac.jp*).
[2] **Current address:** Department of Biofunctional Imaging, Immunology Frontier Research Center, Osaka University, Osaka, Japan.

Cerebral hyperperfusion after carotid endarterectomy (CEA) is defined as a substantial increase in ipsilateral cerebral blood flow (CBF) after surgical repair of carotid stenosis that is well above the metabolic demands of brain tissue (1,2). Cerebral hyperperfusion syndrome after CEA is a complication of cerebral hyperperfusion that is characterized by unilateral headache, face and eye pain, seizure, and focal symptoms that occur secondary to cerebral edema or intracerebral hemorrhage (1–4). Although the incidence of intracerebral hemorrhage is relatively low (0.4%–1.8%), the prognosis for patients with this condition is poor (1,5–9). In addition, results of recent studies (10–12) have demonstrated that post-CEA hyperperfusion, even when asymptomatic, leads to postoperative cortical neural damage and subsequent cognitive impairment.

Risk factors for cerebral hyperperfusion include long-standing hypertension, high-grade carotid stenosis, poor collateral blood flow, and contralateral carotid occlusion, which are all associated with impairments in cerebral hemodynamic reserve (13). Furthermore, a rapid restoration of normal perfusion pressure after CEA may result in hyperperfusion in regions of the brain in which autoregulation is impaired because of chronic ischemia. This hypothesis is similar to the "normal perfusion pressure breakthrough" theory described by Spetzler et al (14) and is consistent with observations by several investigators that decreased cerebrovascular reactivity to acetazolamide or elevated cerebral blood volume is a significant predictor of post-CEA hyperperfusion (15–18).

Magnetic resonance (MR) spectroscopy of the human brain yields a spectrum that includes a large water peak, as well as proton peaks related to *N*-acetylaspartate (NAA), creatines, and cholines (19–22), and human brain temperature (BT) can be calculated noninvasively and accurately from the chemical shift difference between water and NAA, choline, or creatine signals (19–22). In healthy humans, BT is determined by the balance between heat produced by cerebral energy turnover and heat removal (23). Because heat removal is primarily dependent on CBF (23), reduced cerebral perfusion relative to cerebral metabolism, termed "misery perfusion," in patients with acute or chronic cerebral ischemia may indicate decreased central heat removal (ie, higher BT) (22,24). This is supported by observations from a recent study (24) that revealed that BT as measured with proton MR spectroscopy enabled detection of elevated cerebral blood volume and elevated oxygen extraction fraction with high sensitivity and specificity in patients with chronic unilateral major cerebral artery steno-occlusive disease.

The purpose of the present study was to determine whether BT measured by using preoperative proton MR spectroscopy could help identify patients at risk for cerebral hyperperfusion after CEA.

Advances in Knowledge

- A significant correlation was observed between preoperative difference in brain temperature between cerebral hemispheres measured by using proton MR spectroscopy and increases in cerebral blood flow in the affected hemisphere immediately after carotid endarterectomy.
- Elevated preoperative brain temperature difference was significantly associated with the development of postoperative cerebral hyperperfusion.

Materials and Methods

Patient Population

Between August 2008 and April 2009, 84 patients (74 men and 10 women) with unilateral internal carotid artery (ICA) stenosis (≥70%) and good residual function (modified Rankin disability scale score, 0, 1, or 2) underwent CEA. All 84 patients were prospectively enrolled in the present study. Mean patient age was 67.5 years ± 7.6 (standard deviation) (67.4 years ± 7.5 in men, 68.3 years ± 8.2 in women), with a range of 47–82 years (47–82 years in men, 58–80 years in women). Concomitant disease states and symptoms were recorded. There were 76 patients with hypertension, 33 patients with diabetes mellitus, and 44 patients with hyperlipidemia. While 57 patients showed ischemic symptoms in the ipsilateral carotid territory, 27 patients exhibited asymptomatic ICA stenosis. None of the patients had an altered level of consciousness or restlessness.

All patients underwent preoperative MR angiography of the cervical arteries. The overall average degree of ICA stenosis was 88.0% ± 8.2, with a range of 70%–99%, as per the North American Symptomatic Carotid Endarterectomy Trial (25). None of the patients had stenosis greater than 70% or occlusion in the contralateral ICA. Institutional review board approval and informed consent were obtained.

Implication for Patient Care

- Brain temperature measured noninvasively by using proton MR spectroscopy predicts the development of cerebral hyperperfusion after carotid endarterectomy.

Published online
10.1148/radiol.10090930

Radiology 2010; 256:924–931

Abbreviations:
BT = brain temperature
CBF = cerebral blood flow
CEA = carotid endarterectomy
CI = confidence interval
ICA = internal carotid artery
NAA = *N*-acetylaspartate
ROI = region of interest

Author contributions:
Guarantor of integrity of entire study, K.O.; study concepts/study design or data acquisition or data analysis/interpretation, all authors; manuscript drafting or manuscript revision for important intellectual content, all authors; manuscript final version approval, all authors; literature research, T.M., Y.Y., D.I., K.A., K.Y.; clinical studies, T.M., K.O., D.I., M.S., K.K., K.A., M.K., A.O.; statistical analysis, K.O., Y.Y., D.I., H.N., M.K., K.Y.; and manuscript editing, K.O., Y.Y., D.I., M.S., K.K., H.N., A.O.

Authors stated no financial relationship to disclose.

Figure 1

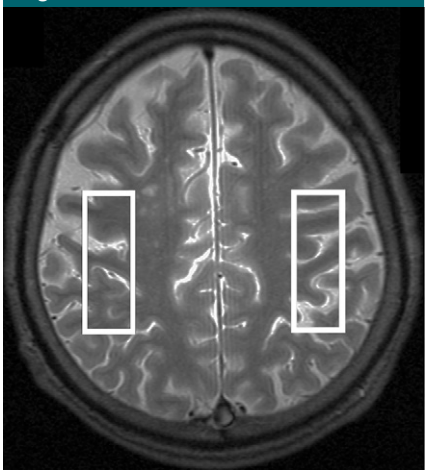

Figure 1: ROIs placed on axial short inversion time inversion-recovery MR image to obtain BT by using MR spectroscopy in 79-year-old man with symptomatic right ICA stenosis (95%) who exhibited hyperperfusion syndrome after CEA. Preoperative ΔBT (BT in affected hemisphere minus BT in contralateral hemisphere) calculated by using the ROIs was +1.15.

Figure 2

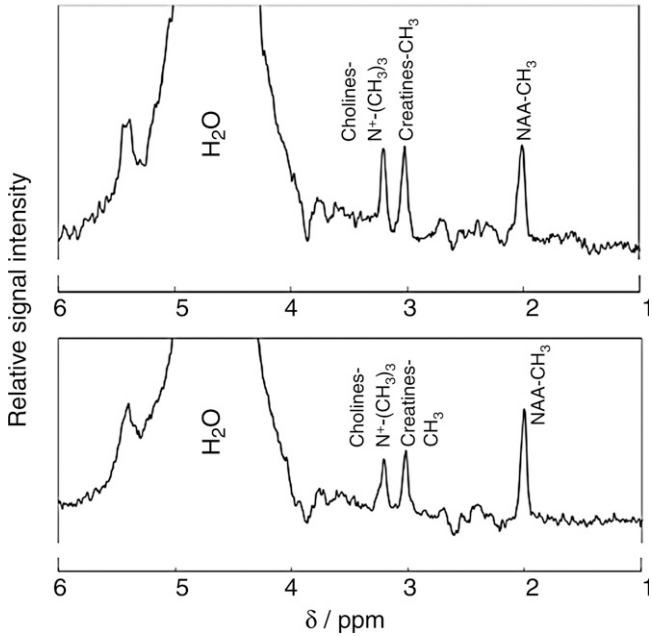

Figure 2: Proton MR spectra obtained by using point-resolved spectroscopy without water suppression in the ROIs in Figure 1. Upper graph: Spectrum in the cerebral hemisphere ipsilateral to that treated with surgery. Lower graph: Spectrum in the contralateral cerebral hemisphere.

BT Measurements at MR Spectroscopy

This study utilized a 3.0-T imager (Signa Excite HD; GE Healthcare, Milwaukee, Wis) with a "birdcage" quadrature head coil. First, all patients underwent axial short inversion time inversion-recovery imaging. From among sections obtained through the centrum semiovale, the section with the thickest white matter was selected. A single-voxel region of interest (ROI) was manually and symmetrically placed in the cerebral cortex parallel to the white matter (Fig 1). Voxel size was $17 \times 50 \times 15$ mm^3. Next, acquisition of proton MR spectroscopy data was performed by using point-resolved spectroscopy without water suppression to estimate BT (Fig 2). The following parameters were used: repetition time msec/echo time msec, 2000/144; data size, 4 K; spectral width, 5000 Hz; and 96 acquisitions (3.9 minutes) (24,26,27). During MR spectroscopy, ambient temperature was maintained at 21°–25°C. The MR spectroscopy study was performed within 7 days before CEA.

Raw data from proton MR spectroscopy were transferred to a postprocessing computer (apodization; 1 Hz and fast Fourier transform), analyzed by using the automatic curve-fitting procedure, and decomposed into Lorenzian peak components by using custom software created in house (24,26,27). In MR spectroscopy, a Lorentzian line shape was commonly assumed on the basis of a one-exponential transverse relaxation behavior of the spins. The real part of the signal was thus used to estimate spectral parameters in a line shape fitting analysis (26). BT for each voxel was calculated from the chemical shift difference between water and NAA signals (ΔH_2O − NAA) by using calibration data from Cady et al and Yoshioka et al (19,27), as follows: T (in degrees Celsius) = $286.9 - 94 \cdot (\Delta H_2O - \text{NAA})$, where T is temperature.

The difference between BT in the affected hemisphere and that in the contralateral hemisphere (value in affected hemisphere minus value in contralateral hemisphere) was calculated on each short inversion time inversion-recovery ROI image and was defined as ΔBT.

Prior to the present study, 11 healthy subjects (six men and five women; mean age, 41 years ± 8; age range, 20–61 years) were examined by using the same methods to obtain control values. The control value for ΔBT was −0.01 ± 0.25 when the left and right sides were defined as the affected and contralateral sides, respectively.

CBF Measurements at Single Photon Emission Computed Tomography

CBF was assessed by using *N*-isopropyl-*p*-[^{123}I]-iodoamphetamine and single photon emission computed tomography (SPECT) performed with a ring-type scanner (Headtome-SET 080; Shimadzu, Kyoto, Japan) before and immediately after CEA. In addition, patients with post-CEA hyperperfusion underwent a third CBF measurement performed in the same manner 3 days after CEA.

The *N*-isopropyl-*p*-[^{123}I]-iodoamphetamine SPECT study was performed as described previously (28), and the CBF images were calculated according to the *N*-isopropyl-*p*-[^{123}I]-iodoamphetamine autoradiography method (28,29). One tomographic plane through the centrum semiovale was selected for each patient.

One large irregular ROI was manually drawn in the portion of the cerebral cortex perfused by the middle cerebral artery, as per the atlas developed by Kretschmann and Weinrich (30), and the CBF was determined in each ROI. Three SPECT studies were used to analyze identical ROIs in each subject.

Post-CEA hyperperfusion was defined as a CBF increase of 100% or greater (ie, a doubling) compared with preoperative values, as according to Piepgras et al (1).

Intraoperative and Postoperative Management

All patients underwent surgery with general anesthesia. An intraluminal shunt was not used in these procedures. The mean duration of ICA clamping was 36 minutes, ranging from 28 to 48 minutes. A 5000-IU bolus of heparin was administered prior to ICA clamping.

In all patients with post-CEA hyperperfusion, intensive control of arterial blood pressure between 100 and 140 mm Hg was instituted by using intravenous administration of antihypertensive drugs immediately after SPECT. When CBF decreased and hyperperfusion resolved on the 3rd postoperative day, pharmacologic control of blood pressure was discontinued. However, if hyperperfusion persisted, systolic arterial blood pressure was maintained between 100 and 140 mm Hg through pharmacologic methods. When hyperperfusion syndrome developed, the patient was placed in a propofol-induced coma with profound hypotension (systolic arterial blood pressure, <90 mm Hg). The diagnosis of hyperperfusion syndrome required *(a)* seizure, decrease in level of consciousness, and/or development of focal neurologic signs such as motor weakness and *(b)* hyperperfusion at SPECT performed after CEA without findings of any additional ischemic lesion at postoperative computed tomography (CT) or T1- and T2-weighted MR imaging.

Statistical Analysis

Descriptive data are expressed as means ± standard deviations. Correlations between preoperative ΔBT and postoperative CBF increases (CBF calculated as a percentage of the preoperative value minus 100%) were determined by using a linear regression analysis, a computing regression equation, and a correlation coefficient. The relationship between each variable and the development of post-CEA hyperperfusion at SPECT was evaluated with univariate analysis by using the Mann-Whitney *U* test or the χ^2 test. A multiple statistical analysis of factors related to the development of post-CEA hyperperfusion at SPECT was also performed by using a logistic regression model. Variables with $P < .2$ in the univariate analyses were selected for analysis in the final model. Differences were deemed statistically significant at $P < .05$. The accuracy of preoperative ΔBT for the prediction of post-CEA hyperperfusion at SPECT was determined by using a receiver operating characteristic curve when the relationship between the two was statistically significant. The curve was calculated in increments or decrements of 1 standard deviation from the mean value of ΔBT in healthy subjects. Exact 95% confidence intervals (CIs) of sensitivity, specificity, and positive and negative predictive values were computed by using the binomial distributions.

Results

Eighty-three of the 84 examined patients recovered from surgery without developing new major neurologic deficits. Furthermore, these 83 patients did not exhibit additional ischemic lesions at postoperative CT and MR imaging that included T1- and T2-weighted imaging. The remaining patient, who underwent right CEA, developed a new postoperative neurologic deficit (left hemiparesis) that persisted for more than 24 hours after surgery. MR imaging on the 1st postoperative day revealed infarcts in the cerebral hemisphere ipsilateral to CEA.

Preoperative ΔBT ranged from 1.77 to 1.31. The increase in CBF immediately after CEA ranged from −20% to +20% when preoperative ΔBT was less than 0 and there was no correlation between the two variables; the increase in CBF ranged from −10% to +140% when preoperative ΔBT was greater than 0 and a significant linear correlation was observed between the two variables ($r = 0.763$ and $P < .001$) (Fig 3).

Nine patients (11%) met CBF criteria for post-CEA hyperperfusion at SPECT performed immediately after surgery. The patient with a new major postoperative neurologic deficit and new cerebral infarcts in the corresponding hemisphere at postoperative MR imaging did not exhibit post-CEA hyperperfusion at SPECT. Results of univariate analysis of factors potentially related to the development of cerebral hyperperfusion after CEA are summarized in the Table. The preoperative ΔBT was significantly higher in patients with post-CEA hyperperfusion than in those without. Other variables were not significantly associated with the development of post-CEA hyperperfusion. After eliminating closely related variables in the univariate analyses, the following confounders ($P < .2$) were adopted in the logistic regression model for the multiple analysis: age, symptomatic lesion, degree of ICA stenosis, and preoperative ΔBT. Subsequent multivariate analysis revealed that high preoperative ΔBT was significantly associated with the development of postoperative cerebral hyperperfusion ($P = .006$; 95% CI: .001, .155).

Sensitivity and specificity for ΔBT at the cutoff point lying closest to the left upper corner of the receiver operating characteristic curve for the prediction of post-CEA hyperperfusion were 100% (nine of nine; 95% CI: 66%, 100%) and 87% (65 of 75; 95% CI: 77%–93%) (cutoff point = +0.49: the mean +2 standard deviations of the control value obtained in healthy subjects), respectively (Fig 3). Positive and negative predictive values were 47% (nine of 19; 95% CI: 24%, 71%) and 100% (65 of 65; 95% CI: 94%, 100%), respectively.

Hyperperfusion was not present at the SPECT examination performed on the 3rd postoperative day in seven of the nine patients with hyperperfusion immediately after CEA; these seven patients had uneventful postoperative courses. However, the remaining two patients with cerebral hyperperfusion immediately after CEA experienced persistent hyperperfusion on the 3rd

Risk Factors for Development of Postoperative Cerebral Hyperperfusion at SPECT

Risk Factor	Postoperative Hyperperfusion		
	Yes ($n = 9$)	No ($n = 75$)	*P* Value
Age (y)*	70.2 ± 8.3	67.1 ± 7.4	.148
Male sex	9 (100)	65 (87)	.591
Hypertension	9 (100)	67 (89)	.590
Diabetes mellitus	4 (44)	29 (39)	.733
Hyperlipidemia	3 (33)	41 (55)	.298
Symptomatic lesions	9 (100)	48 (64)	.052
Degree of ICA stenosis (%)*	92.2 ± 5.1	87.5 ± 8.3	.061
Duration of ICA clamping (min)*	35.6 ± 4.2	35.9 ± 5.1	.885
Preoperative ΔBT*	1.03 ± 0.30	−0.09 ± 0.57	<.001

Note.—Unless otherwise specified, data are numbers of patients, with percentages in parentheses.

* Data are means ± standard deviations.

Figure 3

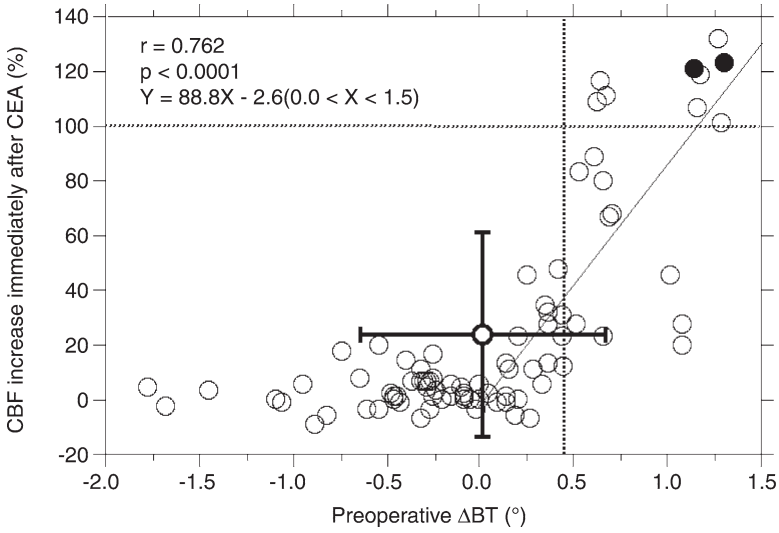

Figure 3: Graph shows correlation between preoperative ΔBT and increase in CBF immediately after CEA. Solid line = function between the two factors, ● = patient who developed hyperperfusion syndrome, horizontal dotted line = CBF increase of 100% (the definition of hyperperfusion), vertical dotted line = mean + 2 standard deviations of ΔBT in healthy subjects, error bar = mean ± standard deviation of each value.

postoperative day and developed the hyperperfusion syndrome. These two patients experienced confusion and hemiparesis, with onset on the 3rd postoperative day in one patient and on the 4th postoperative day in the second patient. Both patients were placed in a propofol-induced coma. The pre- and postoperative SPECT CBF images in one of these patients are shown in Figure 4. Following termination of the propofol-induced coma, both patients eventually experienced full recovery.

Discussion

The results of the present study demonstrated that BT, as measured with preoperative proton MR spectroscopy, can help identify patients at risk for post-CEA cerebral hyperperfusion. Although SPECT with an acetazolamide challenge is a reliable method for predicting cerebral hyperperfusion after CEA (16–18), the clinical use of SPECT is precluded by its high cost and limited availability. In addition, acetazolamide is associated with frequent and various adverse side effects, including metabolic acidosis, hypokalemia, numbness of the extremities, headache, tinnitus, gastrointestinal disturbances, and Stevens-Johnson syndrome (31,32). Studies (15) have demonstrated that measurements of cerebral blood volume at perfusion-weighted MR imaging with gadolinium-based contrast agents also can help identify patients at risk for post-CEA cerebral hyperperfusion. However, contrast agents may be associated with the development of nephrogenic systemic fibrosis in the setting of renal insufficiency (33). Arterial spin labeling and blood oxygen level–dependent imaging are noninvasive MR imaging methods that do not require gadolinium-based contrast agents for perfusion measurement (34,35). However, arterial spin labeling can be used to measure only CBF, and it requires administration of acetazolamide to quantify cerebral perfusion reserve (34). Although blood oxygen level–dependent imaging can help estimate cerebral perfusion reserve (35), whether its findings predict cerebral hyperperfusion after CEA remains unclear. In contrast, the present method does not require administration of radioisotopes or contrast agents and is therefore best suited for clinical use.

Investigators have proposed various mechanisms for the development of post-CEA hyperperfusion (3). In cases of severe ICA stenosis and deficient collateral circulation, hemispheric perfusion pressure is severely reduced distal to the ICA stenosis. This may result in a reduction of perfusion pressure below the compensatory capacity of autoregulatory mechanisms, thus leading to maximal dilatation of resistance vessels and chronic hypoperfusion, or "misery perfusion." After normal perfusion pressure is restored by means of CEA, chronically impaired autoregulatory mechanisms may require several days to adjust to the new steady state, resulting in hyperperfusion in the interim. The present

Figure 4

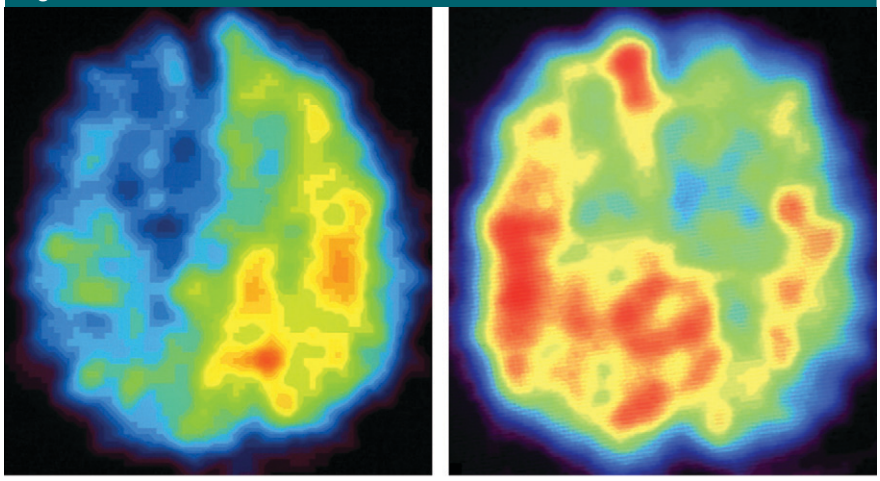

a. b.

Figure 4: SPECT images in same patient as in Figure 1. **(a)** Preoperative image shows a decrease in CBF in the right cerebral hemisphere, in which hyperperfusion is observed on **(b)** image obtained immediately after CEA. This patient developed confusion and left motor weakness 3 days after surgery.

study demonstrated that while there was no correlation between preoperative ΔBT and an increase in CBF immediately after CEA when preoperative ΔBT was less than 0, a significant linear correlation was observed between the two variables when preoperative ΔBT was greater than 0. It also showed that high preoperative ΔBT was the only significant independent predictor of post-CEA hyperperfusion. Because positive and high ΔBT indicates dilation of resistance vessels and misery perfusion in the affected hemisphere (24), our findings support the theory that hyperperfusion results from the loss of normal vasoconstriction secondary to chronic cerebral ischemia and from maladaptive autoregulatory mechanisms.

In the present study, ΔBT had low positive and high negative predictive values for the prediction of post-CEA hyperperfusion; the cutoff point of ΔBT in these values was the mean + 2 standard deviations of the control value obtained in healthy subjects (+0.49°). Furthermore, the cutoff point of ΔBT was identical to that used to detect misery perfusion with a high positive predictive value (24), and the high negative and low positive predictive values in the present study corresponded to previous data obtained by using measurements of cerebrovascular reactivity to acetazolamide at SPECT (16–18). One group (36) reported that most patients with reduced preoperative cerebrovascular reactivity to acetazolamide and hemispheric hypoperfusion during clamping of the ICA developed post-CEA hyperperfusion, suggesting that, in addition to the impairment of cerebrovascular autoregulation caused by chronic ischemia, intraoperative acute global ischemia contributes to the pathogenesis of post-CEA hyperperfusion. This may account for the low positive predictive value for the prediction of post-CEA hyperperfusion when only preoperative measurement of cerebral hemodynamics was used.

The present study had several limitations. First, this study included only patients with unilateral ICA or middle cerebral artery occlusive disease and used the difference in BT between the affected and unaffected sides to help detect hemodynamic impairment in the affected cerebral hemisphere. However, impairments in cerebral hemodynamics are more severe in patients with bilateral major cerebral artery occlusive disease than in those with unilateral major cerebral artery occlusive disease (37), and whole-brain temperature is affected by body temperature but not by ambient temperature (38). Thus, whether cerebral hemodynamic impairment in patients with bilateral major cerebral artery occlusive disease can be detected by using the absolute value of BT remains unclear. Second, the cerebral hemisphere with ICA stenosis often exhibits brain atrophy. In that situation, the proportion of cerebrospinal fluid occupying the ROI used for measurement of BT is high. Cerebrospinal fluid in the ROI may reduce the accuracy of brain tissue temperature measured by using MR spectroscopy. The proportion of the white and gray matter occupying the ROI varies in each subject, which may also affect BT measured in the ROI. Third, physiologic brain motion may cause inaccuracies in metabolite concentration measurements with MR spectroscopy (39). However, the point-resolved spectroscopy technique used in the present study is relatively insensitive to physiologic brain motion (39,40). Because our study cohort did not include any subject with an altered level of consciousness or restlessness, the effects of physiologic brain motion on MR spectroscopy may be negligible (40). Last, BT was measured in a single-voxel ROI placed over the cerebral hemisphere. Although a topographic map of BT can be obtained by using a multivoxel method (22), BT values acquired from a single voxel may provide more accurate MR spectroscopic estimation of brain tissue temperature than those acquired from multiple voxels because the distortion of the spectrum resulting from using a multivoxel method is larger than that resulting from using a single-voxel method (41).

In conclusion, results of the present study demonstrated that BT measured at preoperative proton MR spectroscopy can help identify patients at risk for post-CEA cerebral hyperperfusion. On the basis of findings from the present and previous studies (11,12,15–18), we propose a practical clinical algorithm: Patients undergo preoperative BT measurement performed by using the present method; when this method reveals high ΔBT, patients should undergo postoperative CBF assessments to confirm the development of cerebral hyperperfusion. Furthermore, patients with postoperative cerebral hyperperfusion should

undergo intensive control of blood pressure to prevent development of cerebral hyperperfusion syndrome, which may result in intracerebral hemorrhage or persistent cognitive impairment.

References

1. Piepgras DG, Morgan MK, Sundt TM Jr, Yanagihara T, Mussman LM. Intracerebral hemorrhage after carotid endarterectomy. J Neurosurg 1988;68(4):532–536.
2. Sundt TM Jr, Sharbrough FW, Piepgras DG, Kearns TP, Messick JM Jr, O'Fallon WM. Correlation of cerebral blood flow and electroencephalographic changes during carotid endarterectomy: with results of surgery and hemodynamics of cerebral ischemia. Mayo Clin Proc 1981;56(9):533–543.
3. Bernstein M, Fleming JF, Deck JH. Cerebral hyperperfusion after carotid endarterectomy: a cause of cerebral hemorrhage. Neurosurgery 1984;15(1):50–56.
4. Solomon RA, Loftus CM, Quest DO, Correll JW. Incidence and etiology of intracerebral hemorrhage following carotid endarterectomy. J Neurosurg 1986;64(1):29–34.
5. Dalman JE, Beenakkers IC, Moll FL, Leusink JA, Ackerstaff RG. Transcranial Doppler monitoring during carotid endarterectomy helps to identify patients at risk of postoperative hyperperfusion. Eur J Vasc Endovasc Surg 1999;18(3):222–227.
6. Jansen C, Sprengers AM, Moll FL, et al. Prediction of intracerebral haemorrhage after carotid endarterectomy by clinical criteria and intraoperative transcranial Doppler monitoring: results of 233 operations. Eur J Vasc Surg 1994;8(2):220–225.
7. Ouriel K, Shortell CK, Illig KA, Greenberg RK, Green RM. Intracerebral hemorrhage after carotid endarterectomy: incidence, contribution to neurologic morbidity, and predictive factors. J Vasc Surg 1999;29(1):82–87.
8. Pomposelli FB, Lamparello PJ, Riles TS, Craighead CC, Giangola G, Imparato AM. Intracranial hemorrhage after carotid endarterectomy. J Vasc Surg 1988;7(2):248–255.
9. Riles TS, Imparato AM, Jacobowitz GR, et al. The cause of perioperative stroke after carotid endarterectomy. J Vasc Surg 1994;19(2):206–214.
10. Chida K, Ogasawara K, Suga Y, et al. Postoperative cortical neural loss associated with cerebral hyperperfusion and cognitive impairment after carotid endarterectomy: 123I-iomazenil SPECT study. Stroke 2009;40(2):448–453.
11. Ogasawara K, Kobayashi M, Suga Y, et al. Significance of postoperative crossed cerebellar hypoperfusion in patients with cerebral hyperperfusion following carotid endarterectomy: SPECT study. Eur J Nucl Med Mol Imaging 2008;35(1):146–152.
12. Ogasawara K, Yamadate K, Kobayashi M, et al. Postoperative cerebral hyperperfusion associated with impaired cognitive function in patients undergoing carotid endarterectomy. J Neurosurg 2005;102(1):38–44.
13. Reigel MM, Hollier LH, Sundt TM Jr, Piepgras DG, Sharbrough FW, Cherry KJ. Cerebral hyperperfusion syndrome: a cause of neurologic dysfunction after carotid endarterectomy. J Vasc Surg 1987;5(4):628–634.
14. Spetzler RF, Wilson CB, Weinstein P, Mehdorn M, Townsend J, Telles D. Normal perfusion pressure breakthrough theory. Clin Neurosurg 1978;25:651–672.
15. Fukuda T, Ogasawara K, Kobayashi M, et al. Prediction of cerebral hyperperfusion after carotid endarterectomy using cerebral blood volume measured by perfusion-weighted MR imaging compared with single-photon emission CT. AJNR Am J Neuroradiol 2007;28(4):737–742.
16. Hosoda K, Kawaguchi T, Shibata Y, et al. Cerebral vasoreactivity and internal carotid artery flow help to identify patients at risk for hyperperfusion after carotid endarterectomy. Stroke 2001;32(7):1567–1573.
17. Ogasawara K, Yukawa H, Kobayashi M, et al. Prediction and monitoring of cerebral hyperperfusion after carotid endarterectomy by using single-photon emission computerized tomography scanning. J Neurosurg 2003;99(3):504–510.
18. Yoshimoto T, Houkin K, Kuroda S, Abe H, Kashiwaba T. Low cerebral blood flow and perfusion reserve induce hyperperfusion after surgical revascularization: case reports and analysis of cerebral hemodynamics. Surg Neurol 1997;48(2):132–138.
19. Cady EB, D'Souza PC, Penrice J, Lorek A. The estimation of local brain temperature by in vivo 1H magnetic resonance spectroscopy. Magn Reson Med 1995;33(6):862–867.
20. Corbett RJ, Laptook A, Weatherall P. Noninvasive measurements of human brain temperature using volume-localized proton magnetic resonance spectroscopy. J Cereb Blood Flow Metab 1997;17(4):363–369.
21. Jayasundar R, Singh VP. In vivo temperature measurements in brain tumors using proton MR spectroscopy. Neurol India 2002;50(4):436–439.
22. Karaszewski B, Wardlaw JM, Marshall I, et al. Measurement of brain temperature with magnetic resonance spectroscopy in acute ischemic stroke. Ann Neurol 2006;60(4):438–446.
23. Nybo L, Secher NH, Nielsen B. Inadequate heat release from the human brain during prolonged exercise with hyperthermia. J Physiol 2002;545(pt 2):697–704.
24. Ishigaki D, Ogasawara K, Yoshioka Y, et al. Brain temperature measured using proton MR spectroscopy detects cerebral hemodynamic impairment in patients with unilateral chronic major cerebral artery steno-occlusive disease: comparison with positron emission tomography. Stroke 2009;40(9):3012–3016.
25. Beneficial effect of carotid endarterectomy in symptomatic patients with high-grade carotid stenosis. North American Symptomatic Carotid Endarterectomy Trial Collaborators. N Engl J Med 1991;325(7):445–453.
26. Yoshioka Y, Oikawa H, Ehara S, et al. Noninvasive measurement of temperature and fractional dissociation of imidazole in human lower leg muscles using 1H-nuclear magnetic resonance spectroscopy. J Appl Physiol 2005;98(1):282–287.
27. Yoshioka Y, Shimada R, Oikawa H, et al. Evaluation of noninvasive measurement of human brain temperature using 1H magnetic resonance spectroscopy at 3T. J Iwate Med Assoc 2003;55(5):377–384.
28. Ogasawara K, Ito H, Sasoh M, et al. Quantitative measurement of regional cerebrovascular reactivity to acetazolamide using 123I-N-isopropyl-p-iodoamphetamine autoradiography with SPECT: validation study using H2 15O with PET. J Nucl Med 2003;44(4):520–525.
29. Iida H, Itoh H, Nakazawa M, et al. Quantitative mapping of regional cerebral blood flow using iodine-123-IMP and SPECT. J Nucl Med 1994;35(12):2019–2030.
30. Kretschmann HJ, Weinrich W. Neuroanatomy and cranial computed tomography. New York, NY: Thieme, 1986; 70–74.
31. Derick RJ. Carbonic anhydrase inhibitors. In: Mauger TF, Craig EL, eds. Hevener's ocular pharmacology. 6th ed. St. Louis, Mo: Mosby, 1994.
32. Ogasawara K, Tomitsuka N, Kobayashi M, et al. Stevens-Johnson syndrome associated with intravenous acetazolamide administration for evaluation of cerebrovascular reactivity: case report. Neurol Med Chir (Tokyo) 2006;46(3):161–163.
33. Wiginton CD, Kelly B, Oto A, et al. Gadolinium-based contrast exposure, nephrogenic systemic fibrosis, and gadolinium detection in tissue. AJR Am J Roentgenol 2008;190(4):1060–1068.
34. Zappe AC, Reichold J, Burger C, et al. Quantification of cerebral blood flow in nonhuman primates using arterial spin labeling and a two-compartment model. Magn Reson Imaging 2007;25(6):775–783.

35. Shiino A, Morita Y, Tsuji A, et al. Estimation of cerebral perfusion reserve by blood oxygenation level-dependent imaging: comparison with single-photon emission computed tomography. J Cereb Blood Flow Metab 2003;23(1):121–135.

36. Komoribayashi N, Ogasawara K, Kobayashi M, et al. Cerebral hyperperfusion after carotid endarterectomy is associated with preoperative hemodynamic impairment and intraoperative cerebral ischemia. J Cereb Blood Flow Metab 2006;26(7):878–884.

37. Reinhard M, Müller T, Roth M, Guschlbauer B, Timmer J, Hetzel A. Bilateral severe carotid artery stenosis or occlusion - cerebral autoregulation dynamics and collateral flow patterns. Acta Neurochir (Wien) 2003;145(12):1053–1059.

38. Shiraki K, Sagawa S, Tajima F, Yokota A, Hashimoto M, Brengelmann GL. Independence of brain and tympanic temperatures in an unanesthetized human. J Appl Physiol 1988;65(1):482–486.

39. Pattany PM, Massand MG, Bowen BC, Quencer RM. Quantitative analysis of the effects of physiologic brain motion on point-resolved spectroscopy. AJNR Am J Neuroradiol 2006;27(5):1070–1073.

40. Katz-Brull R, Lenkinski RE. Frame-by-frame PRESS 1H-MRS of the brain at 3 T: the effects of physiological motion. Magn Reson Med 2004;51(1):184–187.

41. Childs C, Hiltunen Y, Vidyasagar R, Kauppinen RA. Determination of regional brain temperature using proton magnetic resonance spectroscopy to assess brain-body temperature differences in healthy human subjects. Magn Reson Med 2007;57(1):59–66.